

Deep insights into MCI diagnosis: A comparative deep learning analysis of EEG time series

Mesut Şeker*, Mehmet Sıraç Özerdem

Department of Electrical and Electronics Engineering, Dicle University, Diyarbakır, Turkey



ARTICLE INFO

Keywords:
 EEG
 Mild Cognitive Impairment
 CNN
 ResNet
 EEGNet
 DeepConvNet

ABSTRACT

Background: Individuals in the early stages of Alzheimer's Disease (AD) are typically diagnosed with Mild Cognitive Impairment (MCI). MCI represents a transitional phase between normal cognitive function and AD. Electroencephalography (EEG) records carry valuable insights into cerebral cortex brain activities to analyze neuronal degeneration. To enhance the precision of dementia diagnosis, automatic and intelligent methods are required for the analysis and processing of EEG signals.

New methods: This paper aims to address the challenges associated with MCI diagnosis by leveraging EEG signals and deep learning techniques. The analysis in this study focuses on processing the information embedded within the sequence of raw EEG time series data. EEG recordings are collected from 10 Healthy Controls (HC) and 10 MCI participants using 19 electrodes during a 30 min eyes-closed session. EEG time series are transformed into 2 separate formats of input tensors and applied to deep neural network architectures. Convolutional Neural Network (CNN) and ResNet from scratch are performed with 2D time series with different segment lengths. Furthermore, EEGNet and DeepConvNet architectures are utilized for 1D time series.

Results: ResNet demonstrates superior effectiveness in detecting MCI when compared to CNN architecture. Complete discrimination is achieved using EEGNet and DeepConvNet for noisy segments.

Comparison with existing methods: ResNet has yielded a 3 % higher accuracy rate compared to CNN. None of the architectures in the literature have achieved 100 % accuracy except proposed EEGNet and DeepConvnet.

Conclusion: Deep learning architectures hold great promise in enhancing the accuracy of early MCI detection.

1. Introduction

Alzheimer's Disease (AD) is a degenerative neurological condition characterized by a gradual decline in memory, communication skills, and the ability to carry out daily activities, including speaking and behavioral disorders. Ultimately, AD results in a fatal outcome. It stands as the predominant form of dementia, accounting for approximately 60–80 % of dementia cases. Generally commencing in middle or late adulthood, it may be triggered by the buildup of proteins around and within neurons, subsequently causing a gradual decline in memory. This decline is linked to synaptic dysfunction, brain atrophy, and neuronal loss (2020 [Alzheimer's disease facts and figures](#), 2020). Brain alterations manifest prior to the onset of cognitive decline, with specific biomarkers displaying abnormal patterns during this early phase. Evidence from research indicates that changes in the brain associated with AD might commence as early as two decades before any noticeable symptoms emerge (Falahati et al., 2014).

Individuals in the early stages of AD are typically diagnosed with Mild Cognitive Impairment (MCI) [4,5]. However, it's important to note that not all MCI patients will progress to AD. MCI represents a transitional phase between normal cognitive function and AD, characterized by subtle cognitive changes that are perceptible to the affected person and their family members, yet the individual remains capable of performing routine daily tasks. Approximately 15–20 % of individuals aged 65 or older experience MCI, and within a span of 5 years, around 30–40 % of those with MCI progress to AD (Prince, 2015). The primary risk factors for AD include a family history of the disease and the presence of relevant genes in an individual's genetic makeup. Diagnosis of AD relies on a clinical evaluation in conjunction with a thorough interview involving both the patient and their family members (Silva et al., 2019). However, it's essential to note that these observations and evaluations might lack accuracy, and objectivity. Furthermore, alongside invasive, and costly biomarkers, diagnostic tools also encompass non-invasive neuroimaging techniques like computed tomography (CT), magnetic

* Corresponding author.

E-mail addresses: mesut.seker@dicle.edu.tr (M. Şeker), sozerdem@dicle.edu.tr (M.S. Özerdem).

M. Seker and M.S. Özerdem

Journal of Neuroscience Methods 403 (2024) 110057

resonance imaging (MRI), and positron emission tomography (PET). However, neuroimaging techniques come with a high cost and are not universally accessible, particularly in remote areas and low-income nations. On the other hand, Electroencephalography (EEG) has emerged as an affordable, non-invasive, and widely available tool, offering valuable biomarkers for diagnosing AD (Perez-Valero et al., 2022). EEG records carry valuable insights into cerebral cortex brain activities, making them essential for studying neuronal degeneration. Nonetheless, visually analyzing EEG signals demands specialized individuals, and their training involves significant time and cost. Moreover, it can be prone to inaccuracies and errors. The manual interpretation of EEG signals is time-consuming, expensive, and subject to human error. To enhance the precision of dementia diagnosis, automatic and intelligent methods are required for the analysis and processing of EEG signals.

This paper aims to address the challenges associated with MCI diagnosis by leveraging EEG signals and deep learning techniques. Early and accurate diagnosis is crucial for effective intervention and treatment. EEG signals offer a unique window into the brain's activities and hold the potential to provide valuable neuro-markers for MCI detection. We propose a novel approach that harnesses the power of deep learning models, including CNN, ResNet, EEGNet, and DeepConvNet, to automatically analyze and classify EEG signals. CNNs excel at learning hierarchical features from raw data, making them well-suited for complex pattern recognition tasks. They automatically extract relevant features, reducing the need for manual feature engineering (Wang et al., 2023). The residual connections in ResNet mitigate the vanishing gradient problem, enabling efficient training of deep models and yielding improved accuracy (Qiu et al., 2023). EEGNet incorporates depth-wise and separable convolutions that efficiently captures both temporal and spatial information in EEG signals, making it highly effective for EEG-based classification tasks (Feng et al., 2022). Finally, DeepConvNet's architecture, comprising multiple convolutional and pooling layers, provides a powerful framework for learning hierarchical features from EEG data (Gemein et al., 2020). Our methodology involves pre-processing the EEG data, preparation of raw input tensors, and training the models on a carefully curated dataset comprising EEG recordings from patients with MCI and Healthy Controls (HC). The analysis in this study focuses on processing the information embedded within the sequence of raw EEG time series data. Temporal analysis of EEG signals is a pivotal aspect of this study, as it provides insights into brain activities over time. This temporal perspective is crucial for distinguishing between HC individuals and those with MCI. Here are the main contributions of this work: i) efficiently capturing and fusing temporal information of EEG signals at varying scales ii) developing both 1D and 2D input modalities for MCI diagnosis iii) providing insights into data preparation for EEG-based MCI diagnosis and highlighting impact of data preprocessing on model performance iv) exhibit robustness of compact models to noise in EEG signals for real-world applications where EEG data may contain various artifacts and disturbances. These contributions collectively advance the use of deep learning for MCI diagnosis, providing a promising avenue for early and accurate detection of this debilitating neurodegenerative condition.

Automatic computer-based diagnosis methods can be broadly categorized into two groups: conventional methods and deep learning-based networks. In both stages, the approaches are distinguished by binary or multi-class classification. The recommended framework for MCI diagnosis encompasses noise reduction, segmentation, feature extraction, and classification, with performance evaluation conducted at the conclusion of the process. Feature engineering relies on extracting specific characteristics from the data to enhance the performance of the model. These characteristics can take the form of i) temporal domain features, ii) frequency domain features (derived from Fourier and wavelet transformations), iii) spatial features (2D activation maps generated from topographic distributions), and iv) connectivity measure matrices indicating relationships between different electrodes (de

Bardeci et al., 2021). Using automated feature learning techniques, like deep learning, can be more practical and effective, as they can adapt to the data's complexity and learn relevant features without the need for extensive manual engineering.

Numerous recent studies have concentrated on leveraging deep learning techniques for the extraction of informative features and subsequent classification of EEG signals. Kim and Kim (2018) collected EEG recordings from 10 HC and 10 MCI participants using 32 electrodes during a 1-minute eyes-open session, with a sampling frequency of 500 Hz. They employed a Deep Neural Network (DNN) for the analysis. By segmenting the data into 2-second epochs and extracting relative power features for all channels in theta, alpha, and beta frequency bands, they obtained a total of 96 (32×3) features. The proposed DNN architecture, utilizing four hidden layers, achieved promising results, with a classification accuracy of 75 % for distinguishing between the HC and MCI groups (Kim and Kim, 2018). Alvi et al. (2022) conducted an analysis of the raw EEG data used in the current work. They employed machine learning algorithms, including Long Short-Term Memory (LSTM), Gated Recurrent Unit (GRU), k-Nearest Neighbor(k-NN), and Support Vector Machine (SVM), utilizing epochs of 6 s. The pre-processing steps involved noise removal, segmentation, and sub-sampling. The segmentation of the provided segments is considered advantageous for increasing the sample size without skipping any instances. For the classification of HC and MCI participants constituting the relevant dataset, a deep learning approach based on LSTM and GRU was employed for the first time. Features extracted by LSTM were subsequently classified by k-NN and SVM for efficiency. A k-fold cross-validation with $k = 5$ was implemented for partitioning the training and test sets. The highest performance was achieved with GRU, obtaining an accuracy rate of $95.51\% \pm 3.11$. Following this, LSTM ($95.47\% \pm 1.17$), DVM ($92.31\% \pm 2.04$), and k-NN ($80.85\% \pm 1.78$) were observed (Alvi et al., 2022). Imani (2023) processed EEG recordings from 24 HC and 24 AD participants using 19 electrodes during a 8 s eyes-open and closed sessions, with a sampling frequency of 128 Hz. Author carried out diverse experiments in various scenarios, encompassing the use of a single common channel (F7), 1 selected channel with the highest entropy, 5 selected channels, and all 19 channels. These experiments were conducted in 2 distinct settings, one without data augmentation and the other with data augmentation incorporated into the analysis. The utilization of Bidirectional Long Short-Term Memory (BiLSTM) networks enables the thorough analysis of time sequences, while the Convolutional Neural Network (CNN) is adept at uncovering intricate relationships among EEG signals captured by diverse channels situated in distinct regions of the brain. Moreover, author introduced an innovative approach referred to as the LSTM and CNN (LMCN) fusion framework. This combination of methodologies allows for a comprehensive examination of both temporal and spatial aspects of the EEG data, contributing to a more holistic understanding of the underlying neural activities. As a result, 98 % acc. was obtained using 5 selected channels with data augmentation via LMCN (Imani, 2023).

The structure of this paper is organized as follows: In the Materials and Methods section, we provide a detailed description of the data collection, preprocessing, and experimental setup, including the deep learning models used for MCI detection from EEG time series. The Results section presents the outcomes of our experiments, including performance metrics, comparisons between different models, and the impact of input modalities. In the Discussion part, we interpret the results, discuss the implications of our findings, and highlight the advantages and limitations of the proposed approach. Finally, the Conclusion section summarizes the key contributions of this work and outlines potential directions for future research in the domain of MCI diagnosis using EEG time series and deep learning.

M. Şeker and M.S. Özerdem

2. Material and methods

2.1. Participants

The dataset in the present study is compiled from participants belong to the study (Kashefpoor et al., 2016), consisting of 11 Mild Cognitive Impairment (MCI) and 16 Healthy Control groups. In order to obtain an equal sample size and balanced data for the relevant dataset, 10 participants are picked up for each group. Balanced representation of different classes prevents the model from being biased towards the majority class. An imbalanced dataset can lead to models that are overly biased towards the majority class, making them less effective when dealing with minority classes. Biases can result in models that perform well on the majority class but poorly on the minority class. In imbalanced datasets, high accuracy may be misleading, as a model can achieve high accuracy by simply predicting the majority class. All participants consisted of individuals aged 60 and above who have received education at the intermediate and higher education levels. The participants are selected from the cardiology unit of Sina and Nour hospitals located in Isfahan, Iran. Individuals with notable psychiatric conditions, medication usage, a history of trauma, severe medical ailments, or advanced-stage dementia are ineligible inclusion criteria. The recruiting process for MCI participants strictly adheres to the Peterson criteria (Weiner and Lipton, 2009). Diagnosis of mild cognitive impairment (MCI) is confirmed using MMSE scores in the range of 21 to 26, with scores exceeding 26 classifying individuals as HC. To confirm the MCI diagnosis and utilize it as the dependent variable, the Neuro-psychiatry Unit Cognitive Assessment Tool (NUCOG) is employed. In the Iranian population, NUCOG scores above 86.5 are considered indicative of normal cognitive status, scores ranging from 75 to 86.5 indicate MCI, and scores below 75 are indicative of dementia. The NUCOG assesses different cognitive functions, including attention, memory, language, and executive function. It may involve tasks such as word recall, attention to detail, and problem-solving. NUCOG can be valuable in identifying cognitive deficits associated with dementia. A lower NUCOG score may indicate cognitive impairment, and a healthcare professional can use this information to further assess the possibility of dementia. MMSE covers various cognitive domains, including orientation, memory, attention, language, and visual-spatial skills. Tasks may include asking the patient to recall information, follow simple commands, and perform basic arithmetic. A lower MMSE score is indicative of cognitive decline. GHQ typically includes questions related to mood, sleep, concentration, and overall psychological well-being. It is designed to identify individuals at risk for mental health disorders. While GHQ is not specifically a dementia screening tool, it can be used to assess the overall mental health of individuals. The demographic characteristics and psychiatric test scores of the participants are summarized in Table 1.

2.2. EEG data records

All EEG recordings are acquired while the participants are comfortably resting in a quiet room with their eyes closed in the morning. EEG recordings are conducted in the morning, with participants in a state of comfortable rest within a quiet, controlled environment with their eyes closed. A total of 19 electrodes, following the 10–20 International sys-

Table 1
Clinical scores and demographics of participants.

	MCI	HC	p
Age (years)	66.4 ± 4.6	65.3 ± 3.9	0.4
Education (years)	10.3 ± 3.8	11.1 ± 3	0.4
GHQ* scores	20.5 ± 9.4	17.9 ± 6.6	0.3
MMSE score	27.6 ± 0.9	29 ± 0.8	< 0.001
NUCOG score	82.4 ± 3.6	91.1 ± 3	< 0.001

* GHQ: General health questionnaire, MMSE: Mini Mental Score Examination

Journal of Neuroscience Methods 403 (2024) 110057

tem, are used for continuous EEG monitoring. These electrodes are intentionally placed at specific locations, including Fp1, Fp2, F7, F3, Fz, F4, F8, T3, C3, Cz, C4, T4, T5, P3, Pz, P4, T6, and O1. The sampling frequency (f_s) is set to 256 Hz, and each recording has a duration of 30 min. While longer recording sessions could potentially reduce variability and minimize noise, they may also lead to a gradual slowing of EEG oscillations due to reduced alertness. Therefore, participants are continuously monitored during the recording process to ensure their sustained wakefulness and prevent drowsiness.

2.3. Methods

In this section of the study, EEG time series are transformed into input tensors and applied to deep neural network architectures. The steps followed in the proposed study are shown in Fig. 1, respectively. Electroencephalogram (EEG) data often faces the challenge of contamination by various artifacts, including but not limited to eye movements (below 4 Hz), cardiac artifacts (around 1.2 Hz), muscle artifacts (above 30 Hz), and the power line effect (50–60 Hz). Independent Component Analysis (ICA) is commonly employed for the removal of eye blinks, muscular movements, and ocular artifacts. However, it has the potential to lead to a notable loss of neuronal data (Mannan et al., 2016). When considering the preprocessing steps in the study where the relevant dataset was obtained are examined, to eliminate artifacts stemming from electrode slippage or subject movement, a visual inspection was conducted, and affected segments were manually excluded, yielding artifact-free signal segments (Kashefpoor et al., 2016). Moreover, filtering might alter the temporal characteristics of the signal. Considering aforementioned circumstances, in proposed study, as a pre-processing step, a 50 Hz notch filter is applied to the EEG recordings to suppress powerline interference (Jiang et al., 2019). Then, a [0.5–32] Hz band-range 4th order Butterworth filter is optionally applied to notch-filtered time series due to its linear response (Daud and Sudirman, 2015). Finally, z-score normalization is applied to the entire dataset, normalizing outliers to have a distribution with a mean of 0 and a standard deviation of 1 (Step 1). The input vectors are prepared in two different forms. The first one consisted of 2D square matrices (Input 1) obtained from EEG segments of varying lengths, while the second involved processing 1D EEG segments by converting them into data format (Input 2) (Step2). The entire dataset has been partitioned into training, validation, and test sets, and subsequently fed as input to deep learning-based architectures. (Step 3). CNN and ResNet from scratch are proposed for Input 1. Moreover, EEGNet and DeepConvNet architectures are performed for Input 2 (Step 4). Then, obtained results are evaluated within performance metrics and confusion matrices (Step 5).

2.3.1. Preparation of input data formats for the architectures

In this stage, EEG recordings from participants are segmented into varying lengths with the aim of achieving the highest classification performance. Accordingly, segments of lengths 4 s, 16 s, and 36 s are selected. The reason for choosing these values was to obtain 2D squared matrices without data loss for creation of Input 1. To create the Input 2 input modality, 30-minute recordings obtained from 19 channels of HC and MCI participants are divided into non-overlapping windows of 2 s each. For a single channel, a total of 900 segments are derived from the entire recording. Consequently, dimensions of different raw EEG modalities are summarized in Table 2 within their corresponding architectures.

In current study, while the number of participants is apparently limited, duration of EEG records (i.e. 30 min) is still satisfactory to extract enough number of EEG segments for further analysis. According to Table 2, we obtained 85500 of (32,32,1), 21280 of (64,64,1), and 9500 of (96,96,1) input vectors for CNN & ResNET. Additionally, we obtained 171000 of (512,1) input vectors for EEGNet & DeepConvNet. The current study is designed as an initial exploration into MCI diagnosis with EEG time series and customized deep learning networks. While we

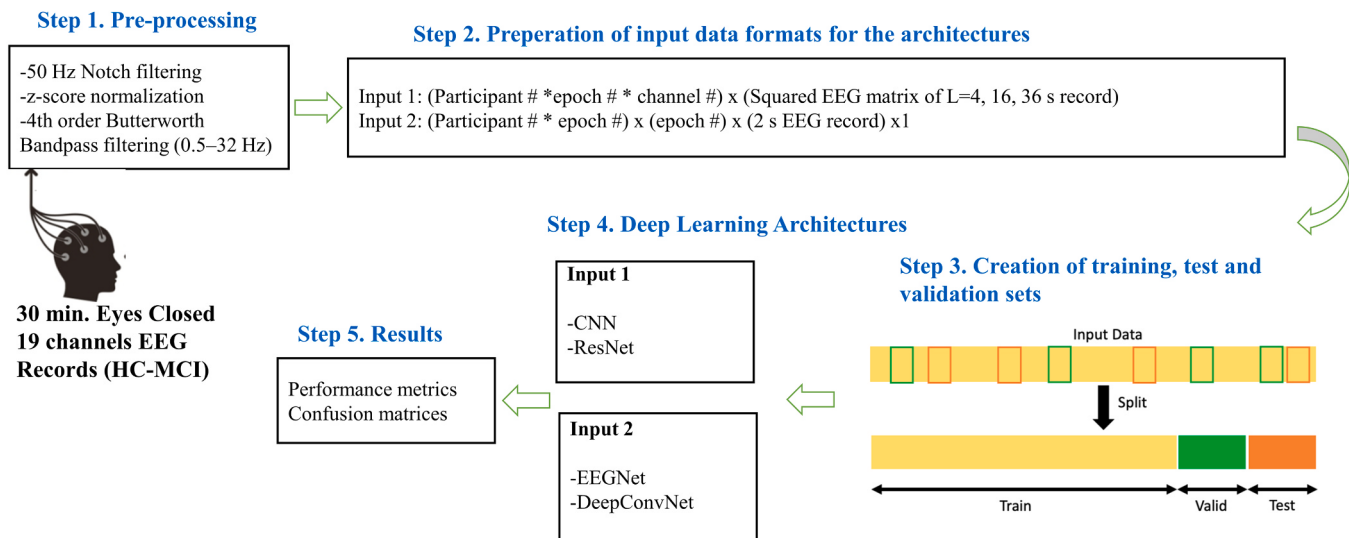


Fig. 1. Steps followed in proposed work.

Table 2

The input vectors for different lengths of segments.

Architecture	EEG Segment Length	Dimensions of input vectors
CNN & ResNet	4 s	((10 par. * 450 seg. * 19 ch.), 32, 32, 1)
	16 s	((10 par. * 112 seg. * 19 ch.), 64, 64, 1)
	36 s	((10 par. * 50 seg. * 19 ch.), 96, 96, 1)
EEGNet & DeepConvNet	2 s	((10 par. * 900 seg.) * 19 ch., 512, 1)

par.: participants, seg. segment, ch.: channel

recognize the limited sample size, it is important to note that our primary aim is to establish the feasibility and preliminary findings in this domain.

2.3.2. Creation of training, test, and validation sets

The process of splitting the data into training and test sets is an essential step in model validation, providing insight into the model's performance on unseen data. During this phase, EEG recordings from individual participants are carefully distributed to ensure that each recording exclusively belonged to either the training, validation, or test set. Initially, the entire input dataset is partitioned into 80 % for training and 20 % for testing purposes. Additionally, a portion of the remaining training data, comprising 20 %, is reserved for the validation process.

2.3.3. Deep neural network architectures for Input 1

2.3.3.1. Convolutional neural network (CNN) from scratch. Within the CNN framework, the feature extraction and classification procedures occur concurrently. Automatic feature extraction is accomplished through a sequence of convolutional stages (i), activation functions (ii), pooling layers (iii) applied to the raw data. Subsequently, the classification task is executed by means of a multi-layer neural network that is fully connected (iv). The convolution stage involves the application of convolutional filters or kernels to the input data, such as images or time series, to extract local features and patterns. These filters slide over the input, performing element-wise multiplications and summations, producing feature maps that highlight specific spatial or temporal characteristics (i). In most cases, the choice of a non-linear transfer function tends to favor the 'sigmoid' or 'hyperbolic tangent' activation functions. However, the 'ReLU' (Rectified Linear Unit) activation function has gained popularity due to its superior performance in terms of generalization ability and faster learning within CNN architectures (ii). Pooling

layers play a crucial role in reducing the resolution or dimensionality of input feature vectors. Their primary purpose is to capture common features effectively. Among pooling techniques, maximum pooling (max-pooling) stands out as an efficient subsampling step that not only enhances generalization performance but also captures salient features (iii). Another critical operation in neural network training is dropout, a technique employed to mitigate overfitting. In dropout, neurons are randomly deactivated during the training process, which introduces an element of uncertainty and prevents the network from relying too heavily on specific neurons. This regularization technique enhances the generalization performance of the network and effectively curbs overfitting. In the fully connected layer, each neuron is connected to every unit in the preceding layer, and the size of the last layer corresponds to the number of classes in the given problem (iv) (Ieracitano et al., 2019).

In the proposed CNN architecture, two convolutional layers are incorporated, each consisting of 64 neurons and (3×3) filters. A (2×2) maximum pooling layer follows each convolutional layer. Subsequently, a fully connected layer with decreasing dimensions of (64, 32) is added, followed by a dropout operation with a 0.3 dropout rate. The activation function used is 'relu,' the loss function is 'binary_crossentropy,' and the optimization algorithm employed is 'Adam. The summary of CNN model parameters is given in Table 3.

2.3.3.2. Residual network (ResNet) from scratch. ResNet, a type of neural network architecture, consists of two consecutive convolutional layer blocks with the same number of filters. The output of the second layer is added to the input of the first convolutional layer (short-cut connection). The number of filters in the input layer must match the number of filters in the final convolutional layer of the module, which is 64. (He et al., 2016). To increase the number of filters in the input layer or decrease the

Table 3

Summary of model layer parameters of Conv2D model for Input 1 size of (96, 96, 1).

No	Layer	Filter no.	Kernel size	Unit	Output
1	Conv2D	64	2	-	$(94 \times 94 \times 64)$
2	MaxPooling2D	64		2	$(47 \times 47 \times 64)$
3	Conv2D	64	2	-	$(45 \times 45 \times 64)$
4	MaxPooling2D	64		2	$(22 \times 22 \times 64)$
5	Flatten				(30976)
6	Dense			64	64
7	Dense			32	32
8	Dropout				32
9	Dense (Sigmoid)			2	2

M. Seker and M.S. Özerdem

number of filters in the final convolutional layer of the module, a solution that can be employed is the use of a 1×1 convolutional layer (Brownlee, 2019). For an example input vector of dimensions (96, 96, 1), the summary of the ResNet architecture is depicted in Table 4.

2.3.4. Deep neural network architectures for Input 2

2.3.4.1. EEGNet. EEGNet was initially developed by Lawhern et al. (2018) with the aim of designing a single generalized CNN for EEG-based Brain-Computer Interface (BCI) applications (Lawhern et al., 2018). EEGNet is a compact model that incorporates depthwise and separable convolution stages in its architecture. These models can be accessed through here (Lawhern et al., 2022). A general EEGNet model is presented in Fig. 2.

Depth-wise convolution plays a pivotal role in CNNs by effectively reducing the number of trainable parameters needed to fit the model. This reduction is achieved by implementing convolutions that are not fully connected to all preceding feature maps. Instead, depth-wise convolution operates on each input channel independently, applying a single convolutional filter to each channel separately (Chollet, 2017). Each input channel is convolved with a different kernel, ensuring that information from different channels remains distinct and doesn't mix in DepthwiseConv2D. Separable convolutions offer significant advantages, primarily centered around (1) the reduction in the number of trainable parameters required to fit the model and (2) the explicit decoupling of relationships within and across feature maps (Howard et al., 2017). Information from different channels is combined in SeparableConv2D stage.

The EEGNet architecture, as defined in Table 5, is characterized by its parameterization, where C represents the number of channels, T stands for the number of time points, F_1 denotes the number of temporal filters, D corresponds to the depth multiplier, signifying the number of spatial filters, F_2 represents the number of pointwise filters, and N indicates the number of classes. This parameterized structure allows for flexibility and adaptability in designing EEGNet models tailored to specific applications and datasets, accommodating variations in the number of channels, time points, filter sizes, spatial filters, pointwise filters, and classes, thereby making it a versatile architecture for EEG-based tasks. In current study, the following parameters are selected for classification of HC/MCI groups: $F_1 = 8$, $D = 2$, $F_2 = F_1 * D = 16$, filter length = 64 (selected up to a maximum of $f_s/2$), drop out = 0.2, and number of epochs during training = 50

2.3.4.2. DeepConvNet. The architecture, consisting of four convolution-pooling layers followed by a classification layer, was developed by Schirrmeister et al. (2017) for application to raw EEG data (Schirrmeister et al., 2017). In this study, (1,5) sized convolution filters, (1,2) sized maximum pooling with a (1,2) stride parameter are utilized. For the classification layer, a 'sigmoid' activation function is chosen due to the binary (HC vs. MCI) classification task. The number of neurons in the convolutional layers of the four blocks is sequentially increased (25, 50,

Table 4

The ResNet model summary using residual blocks for an input vector of dimensions (96, 96, 1).

Type	Layer (type)	Output	Connected to
Input layer	Input_1	(96, 96, 1)	
Conv2D	Conv2d_2	(96, 96, 64)	Input_1
Conv2D	Conv2d_3	(96, 96, 64)	Conv2d_2
Conv2D	Conv2d_1	(96, 96, 64)	Input_1
Add	Add_1	(96, 96, 64)	Conv2d_3
			Conv2d_1
Activation	Activation_1	(96, 96, 64)	Add_1
Flatten	Flatten_1	(589824)	Activation_1
Dense	Dense_1	32	Flatten_1
Dense	Dense_2	2	Dense_1

100, 200). The exponential linear unit ('elu') activation function is employed in these convolutional layers.

3. Results

In this stage, the 30-min. EEG data, acquired from each of the 19 channels for every participant, are transformed into matrices of dimensions 32×32 (corresponding to 4-s epochs), 64×64 (16-s epochs), and 96×96 (36-s epochs). For each 30-min. recording from an individual participant, 450 matrices of size 32×32 , 112 matrices of size 64×64 , and 50 matrices of size 96×96 are generated from a single EEG channel. Considering all participants and 19 EEG channels, a total of ($450 * 10 * 19$) matrices of size 32×32 , ($112 * 10 * 19$) matrices of size 64×64 , and ($50 * 10 * 19$) matrices of size 96×96 are obtained for both the MCI and HC groups. Each test set for the HC and MCI groups contained 17100 matrices of size 32×32 , 4256 matrices of size 64×64 , and 1900 matrices of size 96×96 . These matrices, composed of point-wise EEG records specific to the respective groups, are trained from scratch using CNN and ResNet deep architectures. Prior to classification, the distribution of matrices was updated through z-score normalization.

3.1. Classification of 2D time series of HC-MCI participants using CNN (Input 1)

The matrices containing EEG time series of different dimensions for the MCI and HC groups are trained and tested using the CNN deep neural network architecture, and the results are presented in Tables 6–7. The highest performance is achieved with the 96×96 matrices, with an average accuracy of 0.89.

3.2. Classification of 2D time series of HC-MCI participants using ResNet (Input 1)

When examining the results in Tables 8–9, it is evident that the use of 96×96 matrices as input with the ResNet architecture has led to an improved performance with an average accuracy of 0.92. It can be observed that factors contributing to the increase in accuracy include the larger matrix size and the preference for ResNet, consisting of residual blocks, over CNN.

3.3. Classification of raw HC-MCI EEG time series using EEGNet and DeepConvNet (Input 2)

In this phase of the study, EEG recordings are analyzed in 2-s segments. Each of the HC and MCI groups has tensors of size $19 \times 512 \times 1$, totaling ($10 * 900$) tensors. In the test set, there are 1800 tensors of size $19 \times 512 \times 1$ for each of the HC and MCI groups. During the preprocessing stage, it has been observed that the filtering step improves the performance metrics, and therefore, the results of unfiltered raw data are not included for CNN and ResNet. However, in the case of EEGNet and DeepConvNet algorithms, filtering has the opposite effect on the results. As a result, the results are presented in Tables 10–11, both with and without filtering. In both scenarios, data distribution is updated using z-score normalization. According to Table 10, both algorithms are capable to classify nearly all the EEG recordings of HC and MCI participants correctly without the need for filtering. While quite satisfactory results are achieved with noise-suppressed recordings, it is observed that the filtering process has a negative impact on the results.

4. Discussion

Efficient and precise detection of MCI holds paramount significance in facilitating timely treatment initiation. Early diagnosis of AD assumes a pivotal role in advancing therapeutic interventions and ultimately enhancing the quality of patient care. In traditional machine learning,

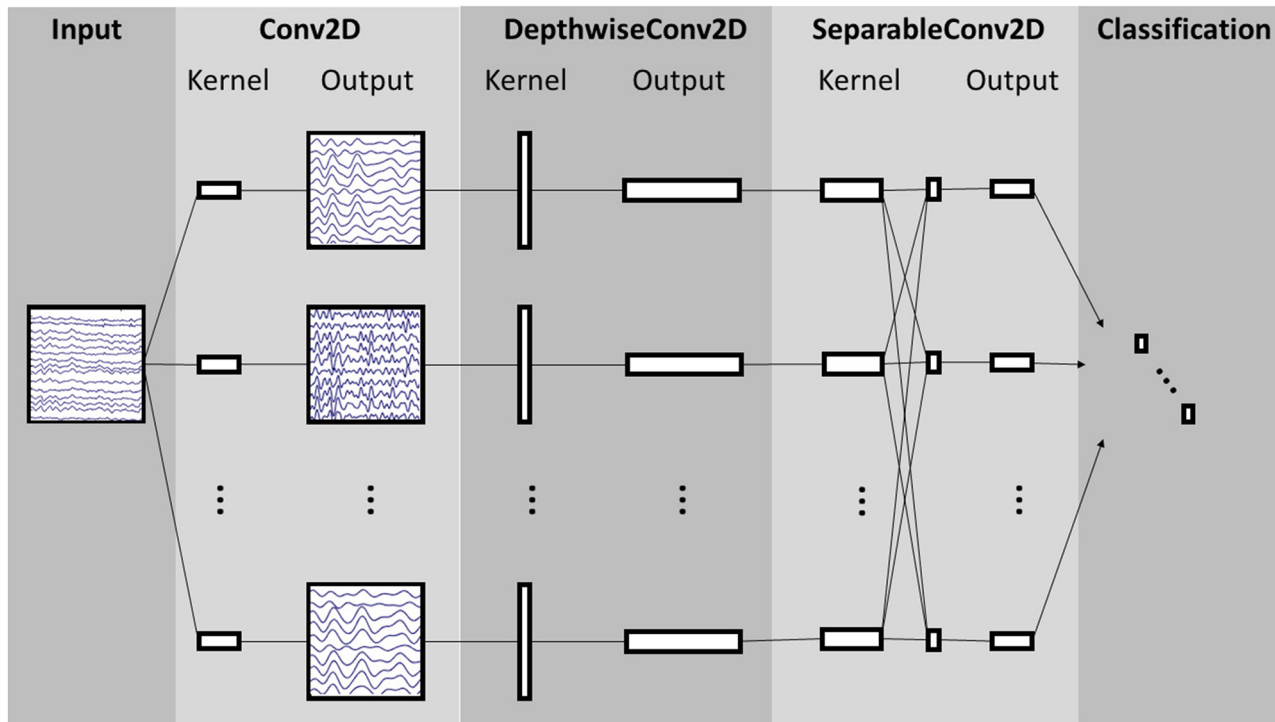


Fig. 2. The structural blocks of the EEGNet architecture (Lawhern et al., 2018).

Table 5

Summary of model layer parameters of EEGNet model for Input 2 with (96, 96, 1) size.

Block	Layer	# filters	Size	# params	Output
1	Input				(C, T)
	Reshape				(1, C, T)
	Conv2D	F_1	(1, 64)	$64 * F_1$	(F_1, C, T)
	BatchNorm			$2 * F_1$	(F_1, C, T)
	DepthwiseCpnv2D	$D * F_1$	(C, 1)	$C * D * F_1$	$(D * F_1, 1, T)$
	BatchNorm			$2 * D * F_1$	$(D * F_1, 1, T)$
	Activation				$(D * F_1, 1, T)$
	AveragePool2D		(1, 4)		$(D * F_1, 1, T // 4)$
	Dropout				$(D * F_1, 1, T // 4)$
2	SeparableConv2D	F_2	(1, 16)	$16 * D * F_1 + F_2 * (D * F_1)$	$(F_2, 1, T // 4)$
	BatchNorm			$2 * F_2$	$(F_2, 1, T // 4)$
	Activation				$(F_2, 1, T // 4)$
	AveragePool2D		(1, 8)		$(F_2, 1, T // 32)$
	Dropout				$(F_2, 1, T // 32)$
	Flatten				$(F_2 * (T // 32))$
	Dense	$N * (F_2 * T // 32)$			N

the performance outcomes are significantly influenced by well-defined features. Nevertheless, as the complexity of the data increases, the process of selecting the most suitable features becomes progressively challenging. In contrast, deep learning possesses the capability to automatically identify optimal features directly from the data. This means that deep learning classifiers can discover and utilize features

that contribute to diagnostic classification without requiring manual intervention.

Table 12 presents a summary of deep learning-based architectures and research methodologies employed in the diagnosis of Alzheimer's disease. The input data for deep learning architectures can be broadly categorized into two components: 1) 1D or 2D point data originating from the signal itself or frequency bands, and 2) The utilization of 2D representations derived from EEG recordings through image transformation techniques. In the literature, point-wise data has been prominently represented either through filtered or noise-affected raw EEG data, with feature extraction applied to create vectors. Additionally, 1D EEG recordings have also been transformed into 2D square tensors for utilization. In the analysis of raw EEG data, there are studies that prefer LSTM and GRU architectures in addition to CNN. In the current study, EEG recordings from MCI and HC groups are transformed into square matrices of sizes 32×32 , 64×64 , and 96×96 with epochs of 4 s, 16 s, and 36 s, respectively. CNN and ResNet architectures are trained from scratch. The highest performance, reaching 92 %, is achieved in the process of training and testing 96×96 matrices using the ResNet architecture. The ResNet architecture, commonly preferred in image-based applications, is adapted in this study to classify 2D square matrices containing point-wise data. In the final part of this stage, EEGNet with depth-wise and separable convolution stages, designed especially for BBA systems, and the DeepConvNet model with consecutive convolution-pooling layers are employed. When reviewing the literature, studies encompassing the use of these models for disease detection in EEG data are rare. The current study processes the utilization of Depth-wise and Separable Convolutions (Chollet, 2016) in EEG signal classification. We have demonstrated that these convolutions can be employed to create an EEG-specific model that incorporates established EEG feature extraction principles. In EEG-specific applications, this operation takes on particular significance as it effectively segregates the task of learning to summarize individual feature maps over time, performed by the depth wise convolution, from the task of optimally combining these feature maps, carried out by the pointwise convolution. This separation is particularly advantageous for EEG signals because various feature maps may represent data at distinct time scales of

M. Seker and M.S. Özerdem

Journal of Neuroscience Methods 403 (2024) 110057

Table 6

Training/validation accuracy-loss graphs and confusion matrices during epochs for squared EEG time series matrices of different input sizes using CNN.

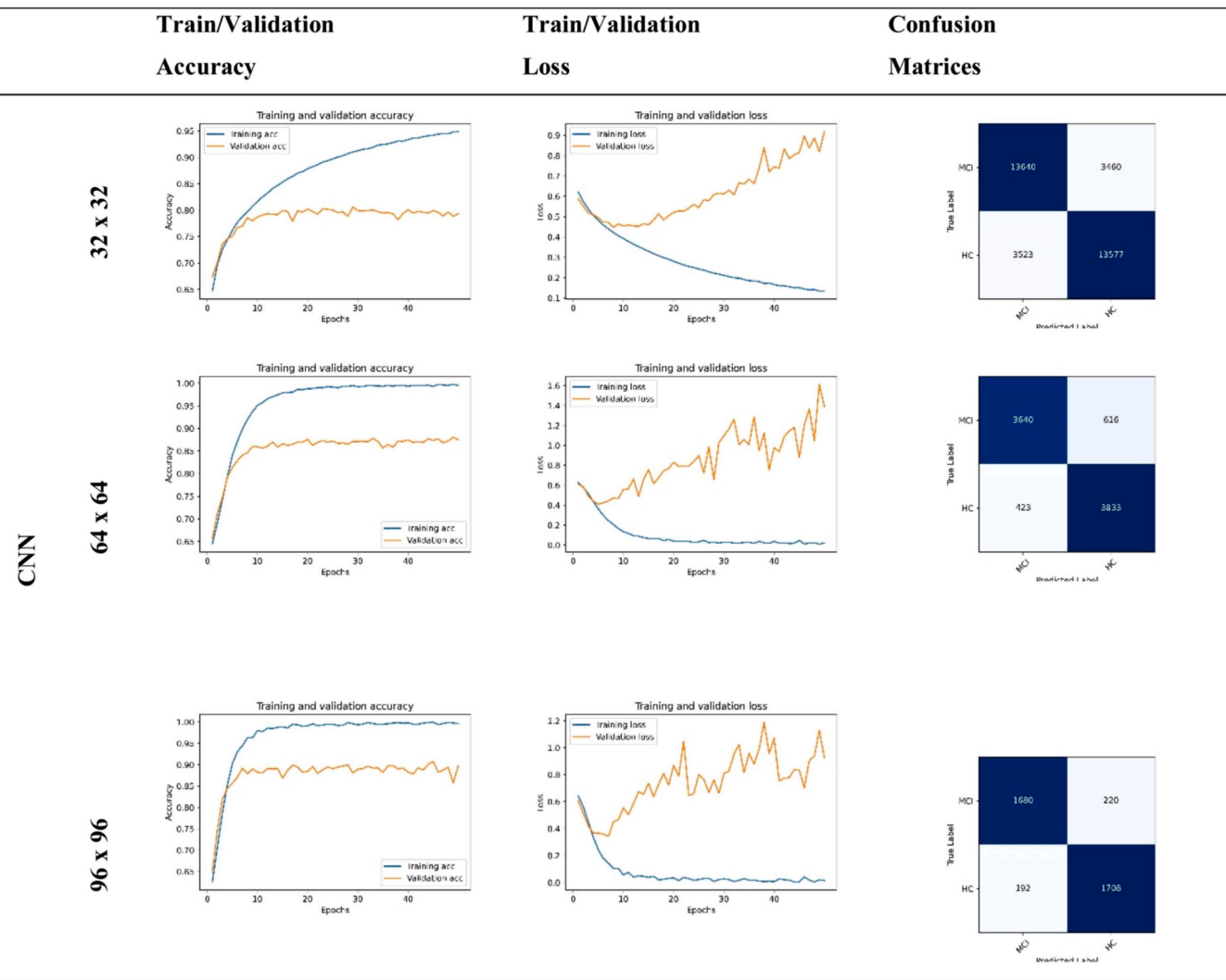


Table 7

Performance metrics obtained in the classification of HC vs. MCI for squared EEG time series matrices of different input sizes using CNN.

Deep Learning Architecture	Input Dimension	Groups	Prec.	Rec.	f1-score	Ave. acc.
CNN	32 x 32	HC	0.80	0.79	0.80	0.80
		MCI	0.79	0.80	0.80	
	64 x 64	HC	0.86	0.90	0.88	0.88
		MCI	0.90	0.86	0.88	
	96 x 96	HC	0.89	0.90	0.89	0.89
		MCI	0.90	0.88	0.89	

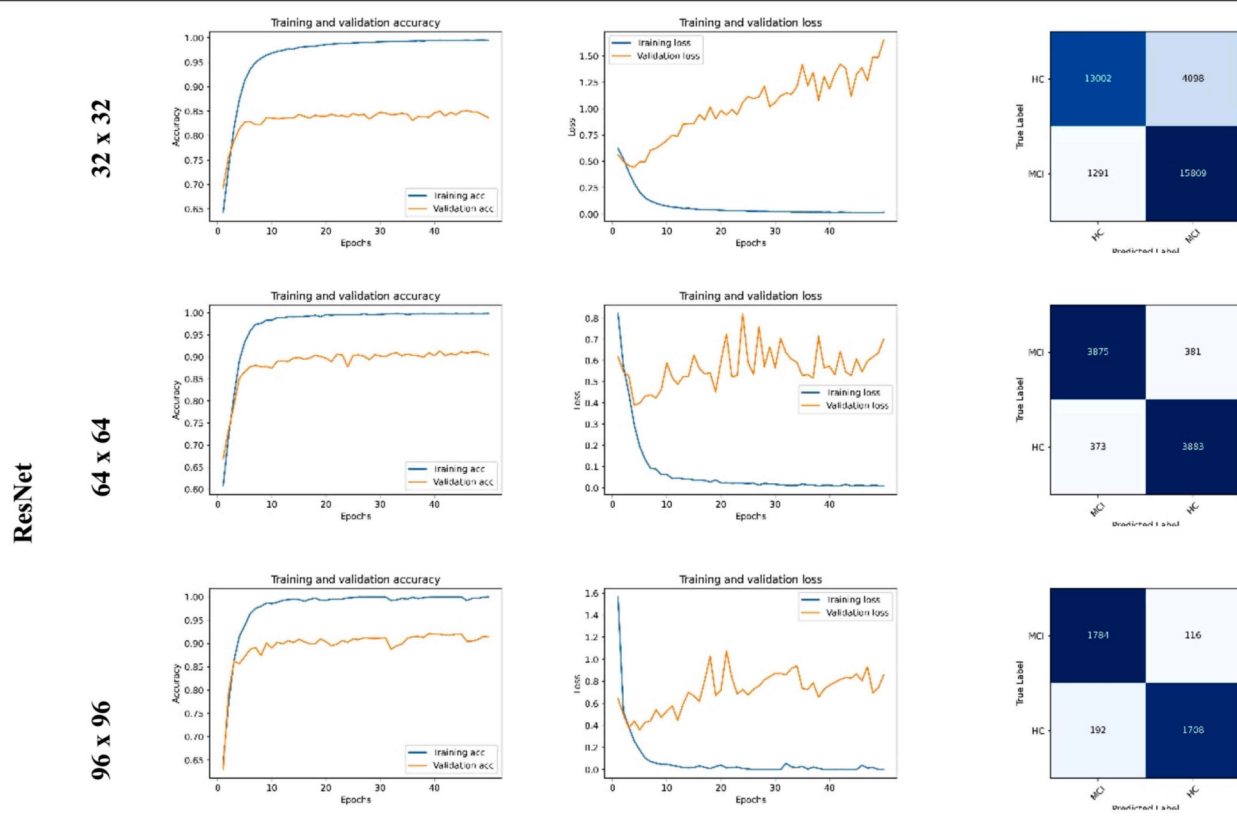
information. By disentangling these processes, the model can efficiently capture and fuse temporal information at varying scales, enhancing its ability to analyze EEG data effectively. The critical aspect here is to prepare input data in accordance with the working principles of the respective architectures. In this study, epochs of 2 s are prepared as input vectors in the format $(10 \times 900) \times 19 \times 512 \times 1$. All epochs from HC and MCI participants are classified with 100 % accuracy.

The methodological novelties and advantages in current study are described explicitly and compared with competitive strategies as following:

- Novel input modalities:** In this study, the preparation of 1D and 2D raw time series in various input forms is demonstrated, as an alternative to computationally demanding image transformation techniques (i.e. spectral images) for EEG.
- Efficient deep architectures:** According to our knowledge, the ResNet architecture, typically employed for image classification problems as an alternative to CNN architecture, has been utilized for the first time in the analysis of time series data. Moreover, the EEGNet and DeepConvNet architectures have been employed for the first time in the analysis of EEG time series data for the purpose of dementia detection. Depth-wise and separable convolution-based networks serve as a viable alternative to LSTM and GRU-based models.
- Preprocessing:** Z-score normalization emerges as an effective preprocessing step in achieving high accuracy. Striking the right balance between noise reduction and information preservation is crucial. We initially experimented many alternatives and came up with the combination of notch filtering and 4th order Butter-worth bandpass filtering for accurate results. Furthermore, EEGNet and DeepConvNet can discriminate between all MCI and HC participants without the need for any filtering. This approach provides an opportunity to completely eliminate the necessity for filtering.
- Sample size:** Equal-sized participant selection is recommended. An imbalanced dataset can lead to models that are overly biased towards

Table 8

Training/validation accuracy-loss graphs and confusion matrices during epochs for squared EEG time series matrices of different input sizes using ResNet.

**Table 9**

Performance metrics obtained in the classification of HC vs. MCI for squared EEG time series matrices of different input sizes using ResNet.

Deep Learning Architecture	Input Dimension	Groups	Prec.	Rec.	F1-score	Ave. acc.
ResNet	32 × 32	HC	0.91	0.76	0.83	0.84
		MCI	0.79	0.92	0.85	
	64 × 64	HC	0.91	0.91	0.91	0.91
		MCI	0.91	0.91	0.91	
	96 × 96	HC	0.94	0.90	0.92	0.92
		MCI	0.90	0.94	0.92	

the majority class, making them less effective when dealing with minority classes.

ResNet, especially proposed to address the problem of gradient vanishing as the depth of neural networks increases, is a significant advancement. In traditional CNNs, performance may degrade when gradients begin to vanish during backward propagation. ResNet employs residual blocks to tackle this gradient vanishing issue. These blocks enable better gradient propagation by adding the network's output to the output of the previous layer. Consequently, deeper networks can be used, resulting in higher accuracy rates. Additionally, ResNet architectures employ shared weights in the network's repeating blocks to reduce the number of parameters. This speeds up the learning process and requires less data. In this study, it has been concluded that using the ResNet architecture is more effective for the time series detection of dementia EEG data with deep learning architectures.

Shorter EEG segments provide higher temporal resolution, capturing rapid changes in brain activity. However, they may not capture long-

term patterns or trends effectively. Longer EEG segments provide a broader context of brain activity, allowing the model to capture more extended patterns and relationships between events. Longer segments may enhance the model's ability to generalize across a wider range of temporal dynamics. While longer segments may improve performance, there is a trade-off with computational efficiency. Researchers need to consider this balance, especially in real-time applications or when dealing with large datasets. EEG data can exhibit significant variability across individuals. The optimal segment size may vary based on individual differences. When processing raw data, it has been observed that increasing the input tensor size (from 32 × 32 to 96 × 96) resulted in improved performance. This finding indicates that using a sufficiently long segment length (36 s instead of 4 s and 16 s) allows for the capture of discriminative patterns between the MCI and HC groups. CNNs derive their learning capacity from their capability to autonomously extract complex feature representations from raw data. Nevertheless, as these features are not manually designed, achieving interpretability in models becomes a considerable challenge. This becomes particularly evident when CNNs are applied to EEG data analysis, as features extracted from neural signals are frequently non-stationary and susceptible to noise artifacts (Nguyen et al., 2015). When all HC and MCI participants' data are prepared in Input 2 modality without any filtering and classified using EEGNet and DeepConvNet, complete discrimination is achieved. The results demonstrate that EEGNet can extract interpretable dementia features, supporting the network's performance and confirming that it is not influenced by noise or artifact signals in the data. The ability to extract neurophysiological features from EEGNet enhances the clinical relevance of the models, ensuring that the network's performance is driven by meaningful information rather than noise. However, when bandpass filtering is applied and a similar process is repeated, it has been observed that the performance decreases by approximately 4–6 %.

M. Seker and M.S. Özerdem

Journal of Neuroscience Methods 403 (2024) 110057

Table 10

Training/validation accuracy-loss graphs and confusion matrices during epochs for squared EEG time series matrices of different input sizes using EEGNet and DeepConvNet.

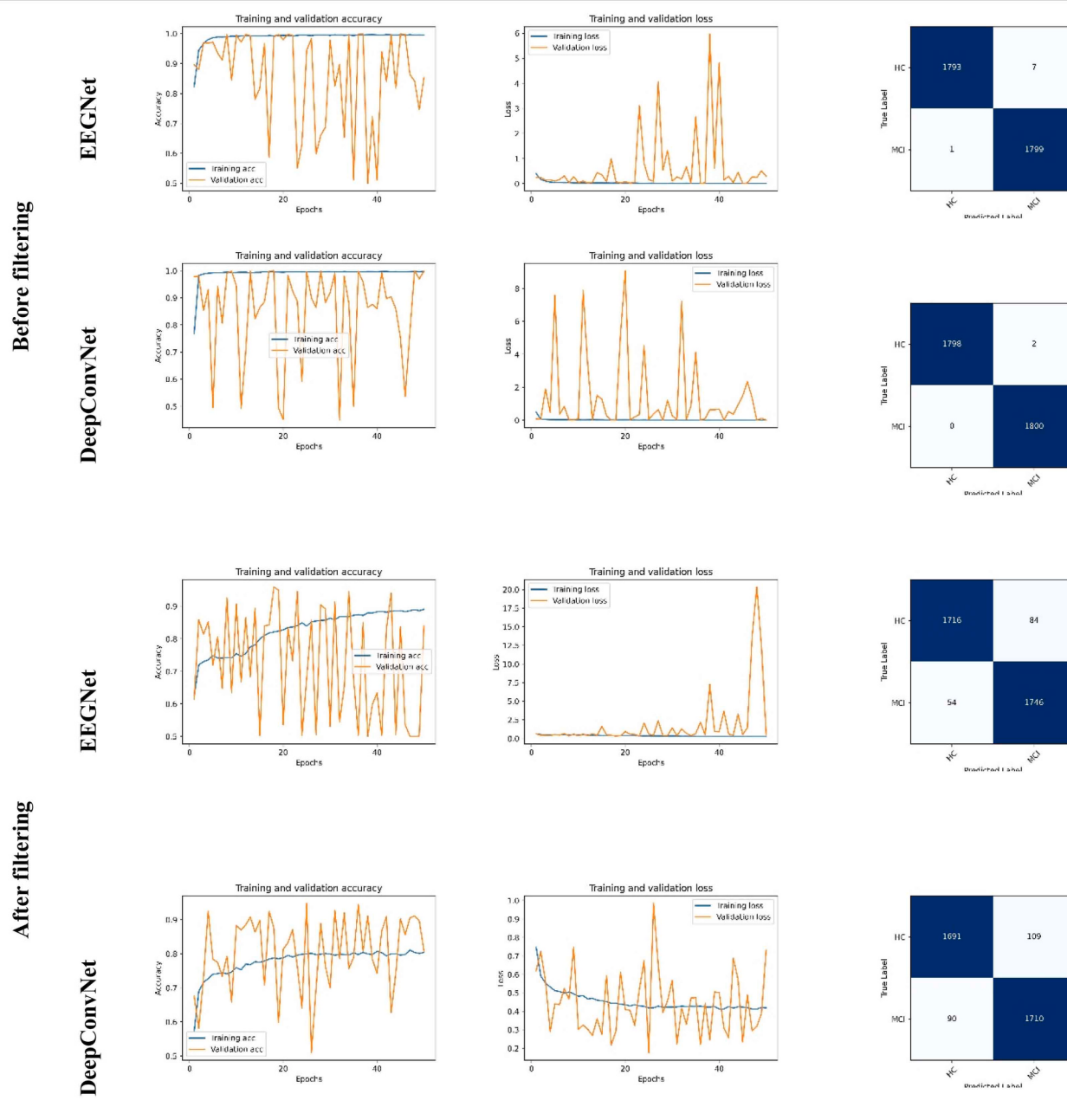


Table 11

Performance metrics obtained in the classification of HC vs. MCI for squared EEG time series matrices of different input sizes using EEGNet and DeepConvNet.

Filtering	Deep Learning Architecture	Groups	Prec.	Rec.	F1-score	Ave. acc.
No	EEGNet	HC	1	1	1	1
		MCI	1	1	1	
No	DeepConvNet	HC	1	1	1	1
		MCI	1	1	1	
Yes	EEGNet	HC	0.95	0.97	0.96	0.96
		MCI	0.97	0.95	0.96	
Yes	DeepConvNet	HC	0.94	0.95	0.95	0.94
		MCI	0.95	0.94	0.94	

While filtering techniques can suppress high-amplitude irrelevant components, they may also inadvertently remove important signal components during this operation. Therefore, in studies, both the positive and negative effects of filtering should be carefully considered, and if necessary, wavelet transform-based filters, which may be more advantageous in the analysis of non-stationary signals, should be used instead of bandpass filters. Filtering might lead to information loss, especially if relevant features are present in frequency bands that are filtered out. EEGNet and DeepConvNet are designed to capture temporal dynamics, and filtering might alter the temporal characteristics of the signal. Both EEGNet and DeepConvNet are known for their robustness in handling raw EEG data. They are designed to capture patterns in the time domain without heavy preprocessing. In conclusion, while EEGNet and DeepConvNet are designed to be robust against noise components

Table 12

Key Literature Studies on Deep Learning-Based Analysis for Alzheimer's Disease with EEG Recordings.

Extracted Features	DL Architecture	Participants	Electrode Number	Records	Epoch Length	Eyes State	Results (acc.)
Complextogram (Polat, 2022)	Lightweight Deep Neural Network (Mobile-Net)	24 HC, 24 AD	19	8 s	2 s	EO-EC	AD vs. HC: 100 % (for Fp2 and F8)
2D RGB spectral topographic maps (Bi and Wang, 2019)	Spiking Convolutional Deep Boltzmann Machine	4 HC, 4 MCI, and 4 AD	64	1 min	1 min	-	AD vs. MCI vs. HC: 9 %
2D gray scale Periodogram Images (Ieracitano et al., 2019)	CNN (with 1 hidden layer)	63 HC, 63 MCI, and 63 AD	19	4.1 min	5 s	EC	AD vs. HC: 91 % AD vs. MCI: 84 % MCI vs. HC: 92 % AD vs. MCI vs. HC: 80 %
2D RGB Mexican Hat CWT Images (Morabito et al., 2016)	CNN (with 2 hidden layer)	23 HC, 23 MCI, and 23 AD	19	-	5 s	EC	AD vs. HC: 85 % AD vs. MCI: 78 % MCI vs. HC: 85 % AD vs. MCI vs. HC: 82 %
2D RGB Scalogram images (Huggins et al., 2021)	AlexNet	52 HC, 37 MCI, and 52 AD	21	10 min	5 s	EC	AD vs. MCI vs. HC: 98.9 %
CWT (Mexican hat) (Fouladi et al., 2022)	4-layer CNN	61 HC, 56 MCI, 63 AD	19	5 min	2 s	EC	CNN: 92 %
Relative Power based features (Kim and Kim, 2018)	AE-CNN	10 HC, 10 MCI	32	1 min	2 s	EO	AE-CNN: 89 %
Raw EEG Dataset (Alvi et al., 2022)	Deep Neural Network (4 hidden layer)	LSTM, GRU, k-NN	19	30 min	6 s	EO	MCI vs. HC: 75 %
EEG Time Series (Imani, 2023)	SVM	RF, SVM, NN, DA, LSTM, CNN, ANN, LMCN	24 HC, 24 AD	19	8 s	EO, EC	MCI vs. HC: 95.51 %
Proposed study 1: Raw EEG 4 s (32 × 32) 16 s (64 × 64) 36 s (96 × 96)	CNN ResNet	10 MCI, 10 HC	19	30 min	4 s 16 s 36 s	EC	CNN: 89 % for 96 × 96 inputs ResNet: 92 % for 96 × 96 inputs
Proposed Study 2: Raw EEG	EEGNet DeepConvNet	10 MCI, 10 HC	19	30 min	2 s	EC	100 % for both EEGNet & DeepConvNet

and can handle raw EEG data effectively, the impact of filtering on their performance depends on various factors, including the filtering method, task requirements, and the specific characteristics of the EEG signals. Striking the right balance between noise reduction and information preservation is crucial, and it often involves careful consideration and experimentation with different filtering strategies.

In proposed study, balanced dataset with equal sample sizes is processed. Moreover, in the train/validation test split, the EEG recordings from individual participants are systematically allocated to ensure that each recording is exclusively assigned to either the training, validation, or test set. For all these reasons, 10 participants are selected for each group of MCI and HC. Class imbalance, where one class has significantly fewer samples compared to others, poses a noteworthy challenge. This imbalance can be addressed through either data augmentation techniques or by reducing the number of original scans from the overrepresented class. The outcomes of experiments conducted with both balanced and unbalanced datasets indicate that accuracy exhibits minor fluctuations based on the class distribution. Interestingly, balancing the dataset, even if it results in a smaller dataset, can lead to performance improvements (Ebrahimpourhaghnavieh et al., 2020).

Despite the success achieved in this study, it is essential to acknowledge certain limitations. The relatively small sample size and the limited exploration of all possible hyperparameter configurations for the deep learning models suggest the need for further investigation with larger and more diverse datasets within more optimal network parameters. Moreover, the interpretability of deep learning models in the context of EEG data remains a challenge, and future research should aim to extract more interpretable features. Furthermore, we highlighted the importance of preprocessing techniques, emphasizing the impact of filtering and normalization choices on model performance. These preprocessing steps significantly contributed to improving the robustness and reliability of our models. The practical approach of analyzing EEG

time series data for MCI detection, as opposed to relying solely on imaging techniques, opens new avenues for research and potential diagnostic improvements. EEG offers the advantage of capturing dynamic brain activity with high temporal resolution. It can detect amplitude changes in neural patterns that might not be observable through imaging alone. This temporal granularity allows for the tracking of cognitive fluctuations and the identification of early-stage MCI, which is characterized by subtle cognitive impairments that may not be evident in static imaging techniques.

5. Conclusion

In a nutshell, this study offers a significant step forward in leveraging deep learning for EEG-based MCI diagnosis. The results suggest that deep learning architectures, particularly ResNet, and EEGNet, hold great promise in enhancing the accuracy of early AD detection. Future research can explore the integration of EEG data with other modalities like MRI, genetic information, or neuropsychological assessments. Combining these diverse data sources can potentially enhance the accuracy of MCI detection models. Analyzing changes in EEG patterns and dynamics over time may offer more accurate predictive models. Developing models that not only detect MCI but also provide interpretable insights into the neural correlates of cognitive decline is crucial. Future studies can focus on creating models that highlight specific EEG features associated with MCI. Collecting and sharing large-scale EEG datasets specifically designed for MCI detection can facilitate benchmarking and the development of robust models. By pursuing these avenues of research, scientists and clinicians can advance our understanding of MCI, improve the accuracy of early detection, and ultimately enhance the quality of life for individuals at risk of cognitive decline.

M. Şeker and M.S. Özdem

Journal of Neuroscience Methods 403 (2024) 110057

CRediT authorship contribution statement

Mesut Şeker: Conceptualization, Formal analysis, Software, Writing - original draft, Visualization; Mehmet Sıraç Özdem: Software, Supervision, Writing - review & editing.

Declaration of Competing Interest

The authors declare that they have no known competing financial interests or personal relationships that could have appeared to influence the work reported in this paper.

Data availability

Data will be made available on request.

Acknowledgement

The authors extend their heartfelt appreciation to The Scientific and Technological Research Council of Turkey (TÜBİTAK) for the generous support through the 2211-C National PhD Scholarship Program in the Priority Fields in Science and Technology, as well as the 2214-A International Research Fellowship Program for PhD Students. Furthermore, this research was funded by Dicle University's Department of Scientific Research Projects, under Project Numbers of MÜHENDİSLİK.20.005 and FBE.21.003.

References

- Alvi, A.M., Siuly, S., Wang, H., Wang, K., Whittaker, F., 2022. A deep learning based framework for diagnosis of mild cognitive impairment. *Knowl.-Based Syst.* 248, 108815 <https://doi.org/10.1016/j.knosys.2022.108815>.
- Alzheimer's disease facts and figures, 2020., Alzheimer's and Dementia. <https://doi.org/10.1002/alz.12068>.
- de Bardeci, M., Ip, C.T., Olbrich, S., 2021. Deep learning applied to electroencephalogram data in mental disorders: a systematic review. *Biol. Psychol.* 162, 108117 <https://doi.org/10.1016/j.biopsych.2021.108117>.
- Bi, X., Wang, H., 2019. Early Alzheimer's disease diagnosis based on EEG spectral images using deep learning. *Neural Netw.* 114, 119–135. <https://doi.org/10.1016/j.neunet.2019.02.005>.
- Brownlee, J., 2019. Deep learning for computer vision image classification, object detection, and face recognition in Python UNLOCK computer vision with deep learning. *Deep Learn. Comput. Vis.* 1–21.
- Chollet, F., 2016. Xception: Deep Learning with Depthwise Separable Convolutions. 2017 IEEE Conference on Computer Vision and Pattern Recognition (CVPR) 1800–1807.
- Chollet, F., 2017. Xception: Deep learning with depthwise separable convolutions. Proceedings - 30th IEEE Conference on Computer Vision and Pattern Recognition, CVPR 2017 2017-Janua, 1800–1807. <https://doi.org/10.1109/CVPR.2017.195>.
- Daud, S.S., Sudirman, R., 2015. Butterworth Bandpass and Stationary Wavelet Transform Filter Comparison for Electroencephalography Signal. Proceedings - International Conference on Intelligent Systems, Modelling and Simulation, ISMS 2015-Octob, 123–126. <https://doi.org/10.1109/ISMS.2015.29>.
- Ebrahimiaghnavieh, M.A., Luo, S., Chiong, R., 2020. Deep learning to detect Alzheimer's disease from neuroimaging: A systematic literature review. *Comput. Methods Prog. Biomed.* 187, 105242 <https://doi.org/10.1016/j.cmpb.2019.105242>.
- Falahati, F., Westman, E., Simmons, A., 2014. Multivariate data analysis and machine learning in Alzheimer's disease with a focus on structural magnetic resonance imaging. *J. Alzheimer's Dis.: JAD* 41 (3), 685–708.
- Feng, L., Yang, L., Liu, S., Han, C., Zhang, Y., Zhu, Z., 2022. An efficient EEGNet processor design for portable EEG-Based BCIs. *Microelectron. J.* 120, 105356 <https://doi.org/10.1016/j.mejo.2021.105356>.
- Fouladi, S., Safaei, A.A., Mamnone, N., Ghaderi, F., Ebadi, M.J., 2022. Efficient deep neural networks for classification of Alzheimer's disease and mild cognitive impairment from scalp EEG recordings. *Cogn. Comput.* 1247–1268. <https://doi.org/10.1007/s12559-022-10033-3>.
- Gemein, L.A.W., Schirrmeister, R.T., Chrabaszcz, P., Wilson, D., Boedecker, J., Schulze-Bonhage, A., Hutter, F., Ball, T., 2020. Machine-learning-based diagnostics of EEG pathology. *NeuroImage* 220, 117021. <https://doi.org/10.1016/j.neuroimage.2020.117021>.
- He, K., Zhang, X., Ren, S., Sun, J., 2016. Deep residual learning for image recognition. Proceedings of the IEEE Computer Society Conference on Computer Vision and Pattern Recognition 2016-Decem, 770–778. <https://doi.org/10.1109/CVPR.2016.90>.
- Howard, A.G., Zhu, M., Chen, B., Kalenichenko, D., Wang, W., Weyand, T., Andreetto, M., Adam, H., 2017. MobileNets: Efficient Convolutional Neural Networks for Mobile Vision Applications. CoRR.
- Huggins, C.J., Escudero, J., Parra, M.A., Scally, B., Anghinah, R., Vitoria Lacerda De Araújo, A., Basile, L.F., Abasolo, D., 2021. Deep learning of resting-state electroencephalogram signals for three-class classification of Alzheimer's disease, mild cognitive impairment and healthy ageing. *J. Neural Eng.* 18 <https://doi.org/10.1088/1741-2552/ac05d8>.
- Ieracitano, C., Mamnone, N., Bramanti, A., Hussain, A., Morabito, F.C., 2019. A Convolutional Neural Network approach for classification of dementia stages based on 2D-spectral representation of EEG recordings. *Neurocomputing* 323, 96–107. <https://doi.org/10.1016/j.neucom.2018.09.071>.
- Imani, M., 2023. Alzheimer's diseases diagnosis using fusion of high informative BiLSTM and CNN features of EEG signal. *Biomed. Signal Process. Control* 86. <https://doi.org/10.1016/j.bspc.2023.105298>.
- Jiang, X., Bian, G.Bin, Tian, Z., 2019. Removal of artifacts from EEG signals: a review. *Sens. (Switz.)* 19, 1–18. <https://doi.org/10.3390/s19050987>.
- Kashefpoor, M., Rabbani, H., Barekatian, M., 2016. Automatic diagnosis of mild cognitive impairment using electroencephalogram spectral features. *J. Med. Signals Sens.* 6, 25–32. <https://doi.org/10.4103/2228-7477.175869>.
- Kim, D., Kim, K., 2018. Detection of Early Stage Alzheimer's Disease using EEG Relative Power with Deep Neural Network, in: 2018 40th Annual International Conference of the IEEE Engineering in Medicine and Biology Society (EMBC). pp. 352–355. <https://doi.org/10.1109/EMBC.2018.8512231>.
- Lawhern, V.J., Solon, A.J., Waytowich, N.R., Gordon, S.M., Hung, C.P., Lance, B.J., 2018. EEGNet: A compact convolutional neural network for EEG-based brain-computer interfaces. *J. Neural Eng.* 15, 1–30. <https://doi.org/10.1088/1741-2552/aace8c>.
- Lawhern, V.J., Solon, A.J., Waytowich, N.R., Gordon, S.M., Hung, C.P., Lance, B.J., 2022. Army Research Laboratory (ARL) EEGModels Project: A Collection of Convolutional Neural Network (CNN) models for EEG signal classification, using Keras and Tensorflow [WWW Document]. URL (<https://github.com/vlawhern/arl-eegmodels>) (accessed 9.12.23).
- Mannan, M.M.N., Jeong, M.Y., Kamran, M.A., 2016. Hybrid ICA—regression: automatic identification and removal of ocular artifacts from electroencephalographic signals. *Front. Hum. Neurosci.* 10, 1–17. <https://doi.org/10.3389/fnhum.2016.00193>.
- Morabito, F.C., Campolo, M., Ieracitano, C., Ebadi, J.M., Bonanno, L., Bramanti, A., Desalvo, S., Mamnone, N., Bramanti, P., 2016. Deep convolutional neural networks for classification of mild cognitive impaired and Alzheimer's disease patients from scalp EEG recordings, in: 2016 IEEE 2nd International Forum on Research and Technologies for Society and Industry Leveraging a Better Tomorrow (RTSI). pp. 1–6. <https://doi.org/10.1109/RTSI.2016.7740576>.
- Nguyen, A., Yosinski, J., Clune, J., 2015. Deep neural networks are easily fooled: High confidence predictions for unrecognizable images, in: 2015 IEEE Conference on Computer Vision and Pattern Recognition (CVPR). pp. 427–436. <https://doi.org/10.1109/CVPR.2015.7298640>.
- Perez-Valero, E., Lopez-Gordo, M.Á., Gutierrez, C.M., Carrera-Muñoz, I., Vilchez-Carrillo, R.M., 2022. A self-driven approach for multi-class discrimination in Alzheimer's disease based on wearable EEG. *Comput. Methods Prog. Biomed.* 220, 106841 <https://doi.org/10.1016/j.cmpb.2022.106841>.
- Polat, H., 2022. Time-Frequency Complexity Maps for EEG-Based Diagnosis of Alzheimer's Disease Using a Lightweight Deep Neural Network. *Traite du Signal* 39, 2103–2113. <https://doi.org/10.18280/ts.390623>.
- Prince, M.A.M.G., 2015. WorldAlzheimer Report 2015-The Global Impact of Dementia: an analysis of prevalence, incidence, cost and trends.
- Qiu, X., Yan, F., Liu, H., 2023. A difference attention ResNet-LSTM network for epileptic seizure detection using EEG signal. *Biomed. Signal Process. Control* 83, 104652. <https://doi.org/10.1016/j.bspc.2023.104652>.
- Schirrmeister, R.T., Springenberg, J.T., Fiederer, L.D.J., Glasstetter, M., Eggensperger, K., Tangermann, M., Hutter, F., Burgard, W., Ball, T., 2017. Deep learning with convolutional neural networks for EEG decoding and visualization. *Hum. Brain Mapp.* 38, 5391–5420. <https://doi.org/10.1002/hbm.23730>.
- Silva, M.V.F., Loures, C., de, M.G., Alves, L.C.V., de Souza, L.C., Borges, K.B.G., Carvalho, M. das G., 2019. Alzheimer's disease: risk factors and potentially protective measures. *J. Biomed. Sci.* 26, 33 <https://doi.org/10.1186/s12929-019-0524-y>.
- Wang, J., Cheng, S., Tian, J., Gao, Y., 2023. A 2D CNN-LSTM hybrid algorithm using time series segments of EEG data for motor imagery classification. *Biomed. Signal Process. Control* 83, 104627. <https://doi.org/10.1016/j.bspc.2023.104627>.
- Weiner, M.F., M Lipton, A., 2009. The American Psychiatric Publishing Textbook of Alzheimer Disease and Other Dementias. American Psychiatric Publishing.